CHEMISTRY OF MATERIALS

ARTICLE

pubs.acs.org/cm

Reversed Phase Composite Polymeric Electrolytes Based on Poly(oxyethylene).

Jarosław S. Syzdek,*[,†,‡,§] Michel B. Armand,[‡] Paweł Falkowski,[†] Magdalena Gizowska,[†] Maciej Karłowicz,[†,‡] Łukasz Łukaszuk,[†,‡] Marek Ł. Marcinek,[†] Aldona Zalewska,[†] Mikołaj Szafran,[†] Christian Masquelier,[‡] Jean M. Tarascon,[‡] Władysław G. Wieczorek,[†] and Zofia G. Żukowska[†]

[†]Warsaw University of Technology, Faculty of Chemistry, ul. Noakowskiego 3, 00664 Warsaw, Poland

[‡]Université de Picardie Jules Verne, Laboratoire de Réactivité et de Chimie des Solides, 33 Rue St. Leu, 80039 Amiens Cedex, France

[§]Ernest Orlando Lawrence Berkeley National Laboratory, Environmental Energy Technologies Division, 1 Cyclotron Road MS70R0108B, Berkeley California 94720-8168, United States

Supporting Information

ABSTRACT: In this paper, a concept and structural characterization of novel class of composite polymeric electrolytes is systematically presented. These are polymer-in-ceramic composites consisting of porous alumina matrices, distinguished by different pore architectures (anodized alumina with narrow and well-ordered parallel pores as well as random structures obtained by various methods from alumina grains by sintering); and a complex of lithium tetraoxochlorate and poly(oxyethylene) of different molecular weight. These new electrolytes exhibit room temperature conductivities exceeding 10^{-3} S·cm^{-1}, low resistance of the interface with lithium electrode, excellent thermal and electrochemical stability. We show combined structural (environmental XRD), thermal and conductivity studies on composite electrolyte systems that were never published before and provide a new explanation of the enhancement of conductivity at subambient temperatures. Feasibility of cells employing electrodes prepared directly on the electrolyte support with a novel synthesis method (MPCVD) is also emphasized.

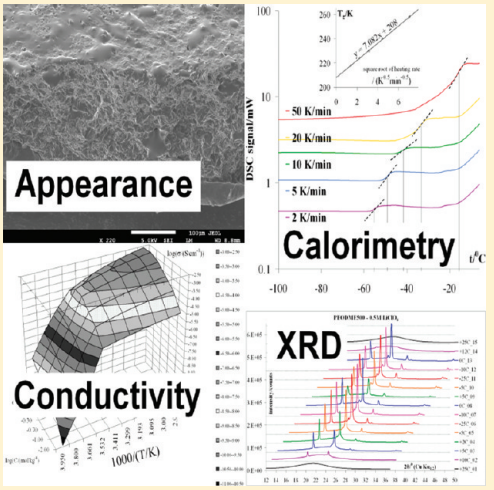

KEYWORDS: characterization of materials, composites, ionic conductors

INTRODUCTION AND CONTEXT DEFINITION

The battery market although satisfied with the success of the Sony technology (intercalation electrodes and organic liquid electrolytes) is facing a great challenge since it is supposed to supply with energy not only portable electronics but also electric vehicles. That adds several factors that become of primary importance although they were considered secondary for small size batteries. First of all safety is an issue. With the present technology overcharge, overheat, or strong mechanical impact (as during an accident) may endanger the user, especially when he or she is sitting on a huge battery pack of the car. Second, one has to keep in mind that the large scale technology should be sustainable, that is, we should be virtually unlimited in resources and able to recycle the materials after use. Addressing the first point, one has to keep in mind that volatile liquid electrolytes[1−7] are to blame for most of the safety issues the present lithium technology has to deal with. On overheat (that can result from either rate charge/discharge, atmospheric conditions or act of vandalism) the liquid contained in the battery can vaporize thus increasing significantly the internal pressure up to levels which may cause cell blow up and release of the solvent. Because of low flash points they can get ignited easily increasing the temperature further and further causing a domino effect leading to consecutive explosions of all cells in the battery pack. Low-temperature overcharge can also be an issue since gases may be released on electrodes simultaneously with lithium plating. Gassing may affect the cell geometry and air-tightness whereas lithium plating may lead to nonuniform deposition in the form of dendrites. These can either cause a short circuit and cell failure (combined with violent heat and toxic products release) or, if they detach from the electrode, lead to the loss of reversible capacity. Furthermore fine lithium particles floating within the electrolyte volume can bring about serious safety issues when they reach positive electrode or when the cell loses its air tightness.

Back in 1972, it was proposed that certain polymers may serve as useful solid solvents for battery electrolytes.[8] Especially poly(oxyethylene) (PEO) was recognized to be most facile material because of its low cost, no toxicity, solubility in many solvents (easy processing), relatively high dielectric constant, high donor number, low glass transition temperature (T_g) leading to high plasticity (good contact with electrodes), substantial viscosity of

Received: October 26, 2010
Revised: February 9, 2011
Published: March 08, 2011

high molecular weight PEO melts allowing the material to withstand creeping at high temperatures, and many others. From the viewpoint of performance it is important to point out that PEO is soft enough to provide good wetting of electrode materials, but at the same time at temperatures below ~80 °C it is still hard enough to stop lithium dendrites from growing into it, thus providing improved safety. However there are some limitations of PEO based electrolytes. First studies by Wright et al., as early as in 1973, showed that this polymer, as well as its complexes with many salts have strong tendency to crystallize, and that the more crystalline the electrolyte, the lower the conductivity.[9] Thus, in order to reach satisfactory performance of a battery, it would have to be kept at temperatures exceeding the melting point of crystalline phases (around 70 °C). For some applications (like electric vehicles) this is not an issue, but for portable electronics this limitation is unacceptable. Hence the high crystallinity of PEO and its complexes was recognized as the main drawback. Furthermore it was found out that the dielectric constant of most polymers is too low to allow full salt dissociation, thus in the electrolyte most of ions remain in aggregated state (ion pairs, triplets, quadruplets, etc.). These aggregates cross-link the polymer chains restricting their mobility and in turn decreasing the conductivity of the material.[10] For many years research on PEO-based electrolytes concentrated on decreasing their crystallinity in order to gain in terms of ionic conductivity. Very often modifications of the material leading to enhanced ionic transport were combined with deterioration of mechanical or electrochemical stability. This will be addressed in more details in the introduction to our second paper. For the moment it is enough to say that one way of polymer electrolytes modification is preparation of composites, that is, enhancing polymer electrolyte conductivity by the introduction of ceramic fillers.[11−13] These can be in the form of powders or fibers. Depending on the filler material, its influence can be different. Attempts to introduce conductive fillers (like β-alumina, NASICON, $LiAlO_2$, Li_3N, and the like[14−21]) failed due to large impedances of the filler−polymer interface. Because of that it was difficult to take advantage of the filler conductivity. Fillers characterized by very high dielectric constant (like $BaTiO_3$[22,23]), when introduced into the polymer may enhance the salt dissociation, provided that the filler grains are large enough to produce ferroelectric domains. All the fillers however, including "inert" materials, such as alumina, titania or silica, affect the properties of polymeric electrolytes by one common mechanism, depending mostly on the filler grain size. When cooling down the polymer melt, huge amount of crystallization centers (each filler grain acting as such) causes rapid growth of poorly developed spherulites, which in turn provoke high amorphicity of the final material. Since the amorphous phase conducts better than the crystalline ones, introduction of fillers increases the conductivity by physical means. However when the filler loading is high, agglomeration and segregation of grains may occur creating obstacles for the ions to move across the electrolyte. Moreover a simple dilution effect further decreases the conductivity (large fraction of insulating phase means low fraction of the conductive polymeric phase[24−27]). For many years different fillers were studied with various success what was a subject of our previous studies that addressed numerous contradictory literature reports in this field and explained both poor and extraordinarily high conductivities of such composites published along last three decades. Difficulties with obtaining materials with uniformly distributed and not agglomerated filler grains were finally overcome, making it possible to study the real effects of the filler on the properties of the final electrolyte, with high reproducibility of the results.[28] In general the observed trend is that the enhancement of the conductivity means deterioration of the mechanical stability. To bypass this limitation, materials built up by two interpenetrating networks started to be studied.[29−43] They used to consist of polymers filled with fibrous fillers as well as polymer−polymer composites based on porous polymer supports. One phase is responsible for the conduction process, and the other is responsible for the mechanical integrity. One has to keep in mind, that when we reach temperatures sufficient to observe high conductivities in polymeric systems, usually they creep at that point. Therefore creating composites with a second phase that remains rigid at cell operating temperatures (and preferably also well above it) is highly recommended for the safety reasons.

Numerous studies were devoted to immobilize polymer electrolytes based on low molecular weight polyethers.[38,44,45] The simplest approach, published by Fedkiw[44] involved the use of nanosized SiO_2. In these systems addition of small fractions of ceramic powder (~5−10% by weight) resulted in formation of gel-type electrolytes with conductivities comparable to those measured for liquid electrolytes incorporated in the silica architecture. A new approach, presented first two years ago, employs polymer-in-ceramic composites that ex definitio offer much better mechanical properties than polymers, ceramic powder-filled polymers, as well as dense and porous ceramics. This is because of their quasi-elasticity at high strains that allow them to be insensitive to brittle cracking, which is the main disadvantage of ceramic materials. Recently very interesting results were obtained in our laboratories regarding such composites of superior mechanical properties.[46] Following first results, we have decided to study in systematic routine these completely new composite polymeric electrolytes. The same concept was studied recently also by Bishop and Teeters.[47] In this paper, we would like to come up with some further details about the relationship between structure and conductivity of such composites that attract more and more attention nowadays. Later on we discuss mechanical properties of such samples and how they correspond to structural data. We also show how these materials can provide improved safety by means of superior thermal and electrochemical stability. Finally, thanks to self-supporting nature of these electrolytes, we used them as supports for electrodes deposition. Preliminary cycling results are provided.

EXPERIMENTAL METHODS

Materials. Several different porous ceramic structures were chosen as supports for the composites preparation. These were alumina based materials with designed pore architecture. Preparation procedure details can be found elsewhere.[48] In short, eight different types of porous alumina specimens were prepared: three by grain sintering of coarse grained alumina powder (ranging from 50 to 80 μm hereafter GS50, GS65, and GS80), one by uniaxial pressing and subsequent sintering of pieces prepared from fine alumina powder (<500 nm, hereafter UA0.5), one prepared from the same fine powder (<500 nm) but with the addition of pore forming agent (microcellulose) that allows designing porosity, pore size and pore architecture in the final material (hereafter OA0.5). Apart from that, commercially available anodized alumina samples were studied. These were Whatman Anodiscs13, 13 mm in diameter, ~50−60 μm in thickness discs, with hexagonally distributed pores of uniform diameter, arterial and perpendicular to the sample surfaces. Pore diameters of these three different types of samples, as

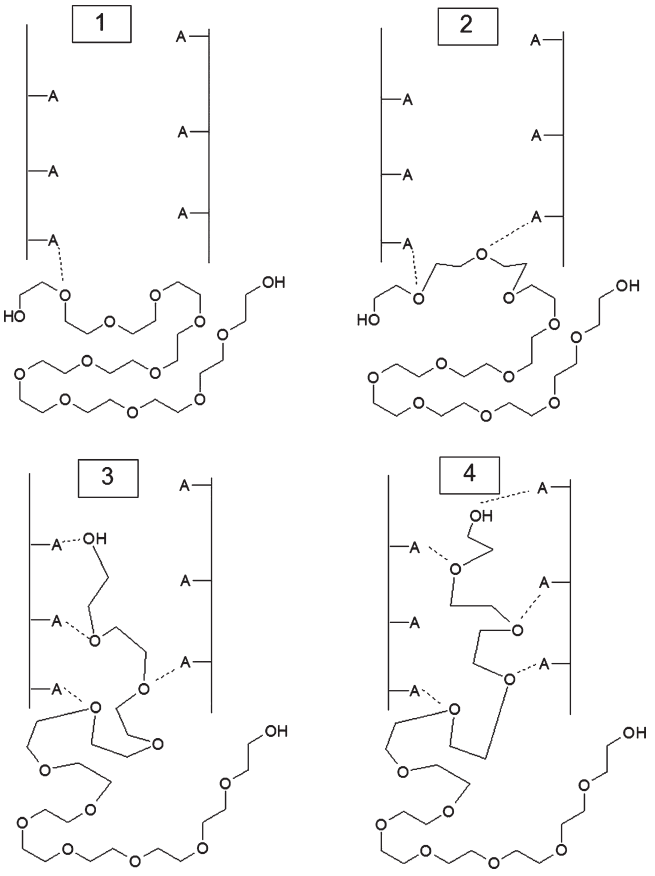

Figure 1. Schematic representation of PEO transport through the pores.

provided by the manufacturer, were 20 nm, 100 nm and 200 nm (hereafter AN0.02, AN0.1 and AN0.2). All materials (ceramics, salt and polymers) were carefully dried (see Supporting Information). We used $LiClO_4$ as a salt. For salt choice judgment consult Supporting Information. We emphasize at this point, that being very cautious about any traces of moisture in composites preparation is fully judged and essential to make the results reliable and meaningful as explained in our recent paper.[28]

Composite Preparation: Low Molecular Weight Polymers. Composites were prepared according to the previously reported procedure.[48]

Composite Preparation: High Molecular Weight Polymers. Application of the procedure described by Bishop was unsuccessful. On pumping argon from above polymer solution in acetonitrile rapid evaporation of the solvent took place and polymer was drying in form of flakes and fibers above the ceramic sample. Stirring appeared not to help the situation at all, and although for thicker samples it was not an issue, for very fine ones, agitation led to breaking of the membranes into little pieces when hit by the magnetic element that was hundreds of times heavier than membranes themselves. Hence after trial and error we elaborated a new, full-proof procedure. At first regular high molecular weight noncomposite electrolytes were prepared according to our previously elaborated procedures with varying salt concentration. Then circular pieces matching the diameter of the ceramic piece were cut and stacked in order to slightly exceed the mass that was expected to fill completely the pores of the ceramic piece (calculated on the basis of dimensions, porosity, and density of the polymer electrolyte). Stacked polymer foils were topped with the ceramic piece itself and the sandwich was placed in a Teflon Petri dish, polymer downward. Petri dish was placed in an airtight chamber inside Ar-filled glovebox, chamber was taken out, evacuated and heated up to 100 °C. Depending on the ceramic piece thickness, it took from two to five days to observe polymer to creep out from the top surface of the ceramic piece meaning that filling the pores with polymer is complete. The mechanism of polymer transport through the pores is presented in figure 1. Its efficiency results from acid−base interactions between ether oxygen (base) and metal (Lewis) or hydroxyl (Brønsted) acid centers (A) present onto the alumina surface (steps from 1 through 4) and great flexibility of PEO chains.

Electrodes and Cells Preparation. Because the conditions of electrodes preparation could damage the polymer, at first electrode material (NiO/C) was deposited onto the ceramic pieces and only afterward polymer was introduced according to the procedures mentioned in the Instrumentation section. Cells were prepared in coin cell (CR2032) and Swagelok configuration. Either blocking (stainless steel) or reversible (lithium metal, Sigma Aldrich) electrodes were used. All manipulations starting from materials preparation ending on disposal of waste were performed in vacuum or controlled atmosphere conditions.

For NiO-C composite electrodes preparation a recently developed method was used, that is, MPCVD. Scheme 1 illustrates for the very first time our novel modified from previously described[49−52] of an apparatus useful for carrying out the method of this invention. Therein depicted is microwave plasma system produced by ERTEC with controlled vacuum programmer system (scheme 1a) produced by β-Erg. System allows precise vacuum control (stabilization and regulation) during the entire reaction time. Vacuum can be programmed during the experiment. Using a reactor according to scheme 1, small amount (∼2 mg) of Nickel(II) acetylacetonate organic precursors (available from Sigma−Aldrich) were placed ∼5 mm from a ceramic substrate (before soaking with the electrolyte) and placed in the plasma chamber. Microwave power not exceed 350W and reaction time were 5 min. The thickness and composition of the Ni-NiO/C film were reproducible and not dependent on the type of substrate. After this process, the electrolyte was introduced into the ceramic piece under vacuum.

Instrumentation. The morphology and surface properties of porous ceramics samples were examined by FEI Quanta 200 Scanning Electron Microscope and JEOL FESEM 7500F, both with EDX analyzer. The accelerating voltage was varied from 1 to 20 kV. Pictures were taken under high and low vacuum (60 Pa of water). Some samples were coated with gold or platinum. Porosity of the samples was determined by hydrostatic method. Ionic conductivity was examined by means of Electrochemical Impedance Spectroscopy in stainless steel blocking electrodes. For that purpose VMP3Multichannel Potentiostat-Galvanostat with Frequency Response Analyzer (Biologic Science Instruments) was employed. Temperature of the samples was controlled by means of HAAKE K75 cryostat-thermostat with HAAKE DC50 temperature controller within 0.03 K precision. Electrochemical cells prepared in Swagelok configuration were placed in a Faraday cage immersed in the cooling/heating bath (see Supporting Information for details). Same procedure/equipment was used for electrochemical stability studies. Cells were studied for over 3 months by means of recording the spectrum each day for each electrolyte.

Lithium ion transference number was examined by means of Electrochemical Impedance Spectroscopy and Direct Current polarization (Bruce−Vincent method) in lithium metal (reversible) electrodes. Same instrumentation as for stability studies was used; in fact exactly the same cells were used. That guaranteed that system is in equilibrium and the only transient phenomena observed are those caused by application of the polarization current. Spectra were recorded in 500kHz-50mHz frequency range with 20 mV peak-to-peak amplitude before and immediately after the polarization step. The latter consisted of 10 mV DC polarization for a period of 20−24 h to ensure the steady state is reached. In fact usually 4−6 h were enough to ensure current decay slower than 1% per hour.

Scheme 1. Scheme of Microwave Plasma System[a]

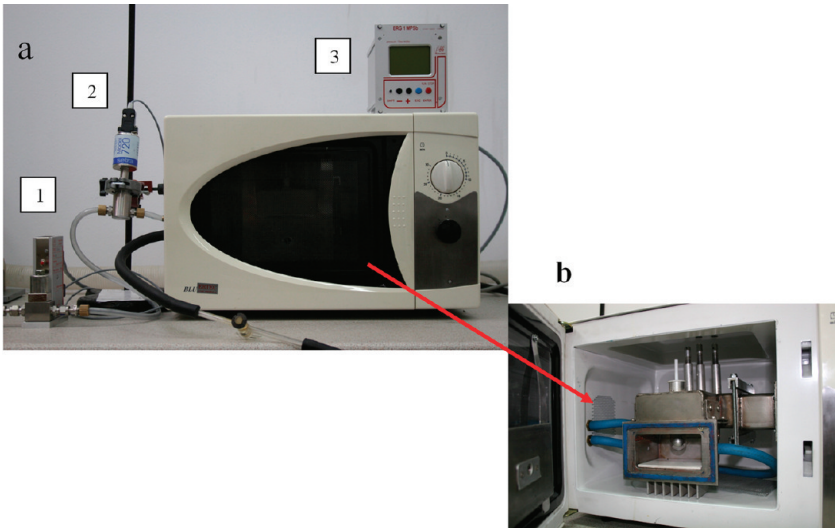

[a] Part a: (1) manual regulation valve, (2) vacuum probe, and (3) vacuum programmer. Part b: Open plasma chamber/resonator.

Electrochemical studies of full cells were conducted with the same VMP3 instrument. At first cycling voltammetry was performed at low scan rate (0.02 mV/s) for determination of the correct potential window for cycling in galvanostatic mode. Then galvanostatic cycling with potential limitation was performed at so-called 1C rate (full capacity delivered in 1 h).

Differential scanning calorimetry measurements were conducted with two different instruments. One was TA Instruments Q200, the other one was Netzsch DSC 204 F1 Phoenix. DSC traces were recorded according to a temperature program: 30 °C → −120 °C → 70 °C → −120 °C → 70 °C → 30 °C in a stream of pure argon. Heating and cooling rates were 5, 10, 20, and 50 K·min^{-1}. Five minutes isothermal steps were separating consecutive temperature ramps. Liquid nitrogen was the coolant. Aluminum pans were used. They were closed inside the drybox, measurements were conducted in a stream of argon. Empty pan (with argon inside) was used as a reference.

X-ray diffraction patterns were recorded with Bruker D8 Diffractometer, working in $\theta-\theta$ geometry. It was equipped with a Cu-anticathode and Ni monochromator (Cu $K_{\alpha 1,2}$). The detector was an energy-filtering, position-sensitive CCD camera (Lynx-Eye). Lower cutoff voltage was 0.11 V; the energy window was 0.14 V. Diffractograms were recorded within 10−60° (2θ) angle range with 0.01° resolution. A low-temperature attachment was employed to control samples temperature. To avoid samples exposure to air, the attachment was transferred to the Ar-filled glovebox, where the samples were mounted on the stage, then it was sealed and attached to the diffractometer. Before recording the diffraction patterns, the sample chamber was evacuated down to around 10 Pa to avoid X-rays absorption by the Ar gas. At each measurement temperature, samples were equilibrated for at least 30 min; then scans were performed twice to observe any changes upon time. In each case, both scans were exactly the same hence they were added to increase the signal-to-noise ratio.

Mechanical properties were studied with TINIUS OLSEN H10KS two column bench machine. Axial compression test (Scheme S1 in Supporting Information) was applied since in the usual configuration of the electrochemical cell, these are both pressing and tearing forces that act on the separator.

Thermal stability was studied by means of simultaneous thermal analysis−mass spectrometry. STA 449 C Jupiter TG-DSC coupled with Quadrupolar Mass Spectrometer 403 Aeolos was used for this purpose. Heating rate was 20 K·min^{-1}, scans were carried out starting at room temperature up to 400 °C.

Raman measurements were made at room temperature on Nicolet Almega Dispersive Raman Spectrometer equipped with confocal microscope, using 780 nm diode laser and 360 grooves/mm grating. Samples were prepared inside the Ar-filled glovebox and studied in an environmental cell.

RESULTS

Ceramic Pieces. Apparent density bore total porosity values. Open porosity of the pieces was determined by hydrostatic method. Among each population of samples, values were nicely reproducible proving that each batch of pieces prepared with a specific method was uniform (Table S1 in Supporting Information). All of the samples were 8.73 mm in diameter, with thicknesses varying from 0.35 to 0.95 mm (each sample was flat). The general observation was that for samples sintered without pore-forming agents, porosity could have been increased from 35% up to 67% when moving from <500 nm to 80 μm alumina grains; however, the mechanical properties of samples with porosities greater than 62% were not satisfying. Samples prepared with organic additives promoting well-defined pores could have been sintered at high temperatures, where intrinsic porosity (intergranular pores) is almost completely lost and only that provoked by the burnt out organic material remains. In this manner even samples with 60% porosity were exceptionally strong. Porosity of commercial anodized alumina pieces was determined to be around 64%. Extended SEM studies are presented in the Supporting Information (Figure S1).

Electrolytes. Before any measurements were taken, excess electrolyte had been removed from the surfaces of ceramic pieces. According to the porosity data and density of electrolytes, complete filling of the pores with electrolytes was confirmed within the balance precision. Filled electrolytes when watched under SEM at subambient temperatures showed complete filling of the pores. X-ray energy dispersive spectra confirmed the presence of electrolyte in the deep parts of samples. Following the weight of samples in an extended period of time (up to two years) revealed that polymer has no tendency to escape from the ceramic matrix.

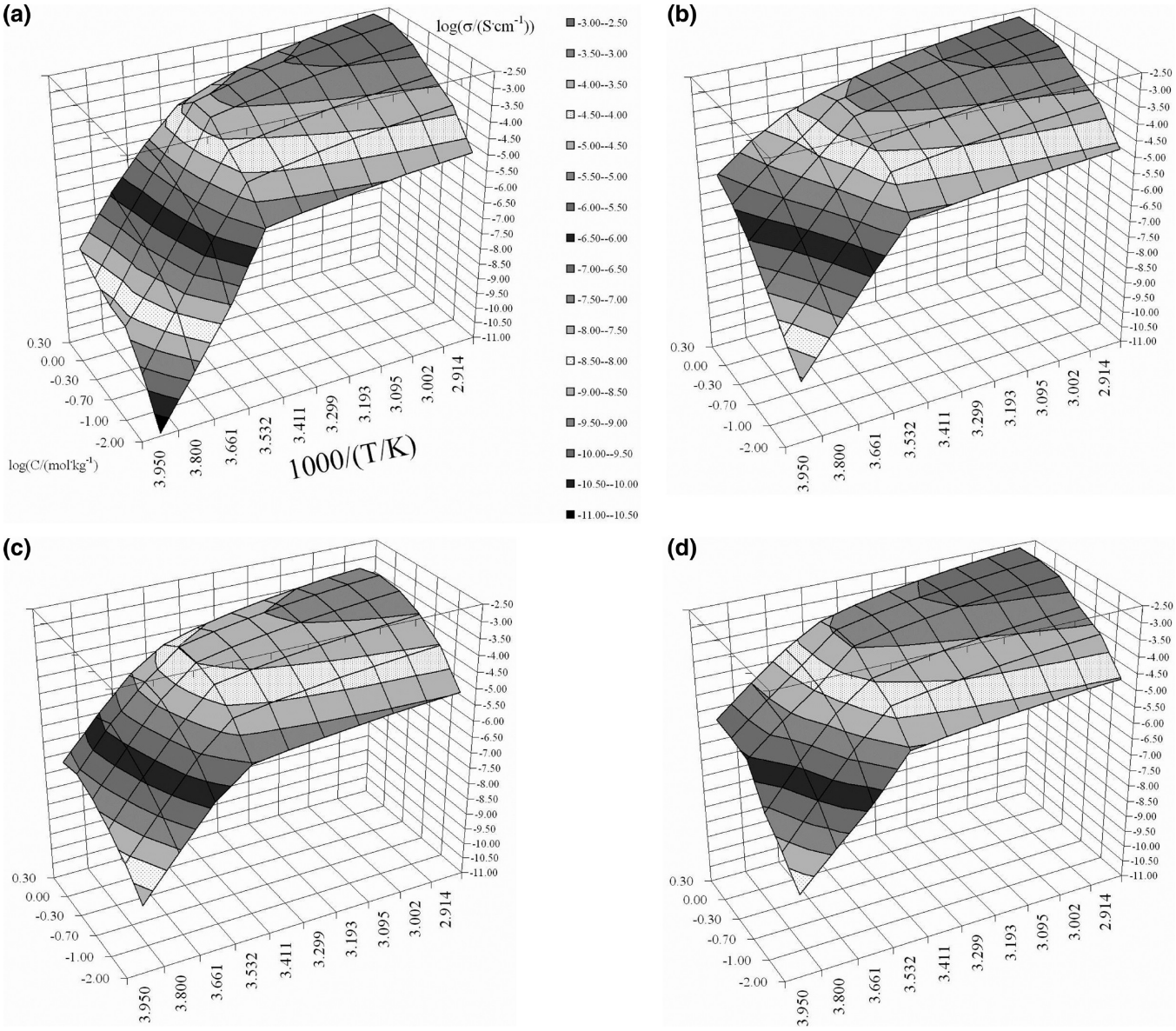

Figure 2. Arrhenius plots of conductivities of several populations of electrolytes. Grayscale codes and axes are consistent for all figures: (a) noncomposite system, (b) composites based on OA0.5 ceramics (large pores), (c) composites based on UA0.5 ceramics (tiny, randomly oriented pores), and (d) composites based on AN0.1 ceramics (100 nm pores, oriented perpendicularly to electrodes).

Conductivity Studies. Conductivity and electrochemical stability of a large population of composite electrolytes was studied together with plain salt-polymer complexes used as references in a wide frequency and temperature range.[53−56] Conductivities were calculated with dimensions of the specific piece that varied from one to another (also in case of the commercial ones) and were NOT corrected by the term including the space occupancy by the conductive phase, that is, the conductivity refers to the sample as a whole, not just the polymer.

Figure 2 (a through d) presents Arrhenius plots of conductivities of several populations of electrolytes (each graph shows data for 6 samples, containing salt at 2.0, 1.0, 0.50, 0.20, 0.10, and 0.010 M concentration, shown on a logarithmic scale, grayscale codes and axes are consistent for all figures). Note how pore size and architecture affects the conductivity profile, and how it depends on the salt concentration. Presence of ceramic (insulating phase) should decrease the total conductivity by a factor of ∼2−3. However, it is not the case, except for UA0.5-based composites (c), where porosity is really low and randomly oriented (high tortuousness). For other samples polymer-salt-ceramic interactions enhance the specific conductivity of the polymer phase to make up for the insulating phase content in the high temperature zone. At low temperatures the influence of ceramic is much more profound. One can clearly tell, that large pores are most efficient at high salt concentrations (b), whereas small pores are more effective at low concentrations (c, d). Furthermore, some degree of order in the pore structure promotes better performance even at high salt concentrations (d). Note that ceramics (b, c, d) flatten the conductivity profile as a function of salt concentration at any temperature above polymer melting point.

Looking in greater details at the Arrhenius plots of the conductivity of salt solutions in PEODME500, one can observe

dx.doi.org/10.1021/cm103021r |*Chem. Mater.* 2011, 23, 1785–1797

slightly bent profile in the high temperature zone, following the VTF or WFL-like behavior[57−61] (Figure 2a). That means that the ionic movement is highly coupled with the motion of polymer chains. As mentioned in the Introduction, PEO exhibits strong tendency to crystallize, therefore on passing the melting point on cooling, in most cases crystallization occurs and poorly conducting crystalline phases appear. In these crystals migration of ions is decoupled from the motion of polymer chains and logarithm of conductivity versus reciprocal temperature profiles become straight lines (pay attention how low are these conductivities). In general, on increasing the salt concentration conductivity increases to reach maximum around 1 mol·kg^{-1} and then decreases. Viscosity of such electrolytes systematically increases with salt concentration and as proven by spectroscopic measurements and appropriate calculations, conductivity decreases abruptly due to aggregation of ions and slower segmental motion of polymer chains.[10,62,63] On the other hand in subambient temperature zone salt concentration corresponding to maximum conductivity is greater because high viscosity of the electrolyte restrains the crystallization in some extent and according to widely accepted model claiming that conductivity takes place mostly in the amorphous phase.

Moving to the composite systems one can observe that in the high temperature zone, the conductivity is close to that of plain salt-in-polymer solution. If one keeps in mind that the conductive phase occupies at most 60% v/v, and in some samples only 35% (which means around 14% w/w), these results are encouraging. In case of classical, powder filled polymers, beyond 50% w/w of filler, conductivity decreases rapidly because of segregation and agglomeration of filler. Moreover at high filler loadings the mechanical integrity of the electrolyte is of question.[19] Here ceramic grains are sintered together and open channels filled with polymer are maintained even at high fractions of insulating ceramic phase. Thanks to the porous structure, a solution of salt in low molecular weight polymer, can be transformed into a material with excellent rigidity modulus, without losing much of its ionic transport abilities. Possibility of providing relatively high conductivity at so low loading of polymer and salt should be considered a great advantage of these systems. Should a complete cell with such electrolyte be thermally abused, the amount of material that can react with electrodes (salt and polymer) is low, furthermore ceramic support will separate oxidizer (positive electrode) from the fuel (negative electrode) and they would decompose separately, without being engaged in a rapid self-discharge.

The main advantage of this kind of systems appears however at sub ambient temperatures that used to be the salt in the eye of polymer electrolyte community. In case of noncomposite systems, crystallization causes abrupt decrease of the conductivity when passing the melting point.[1,2] When the polymer is held within the pores, on cooling one can observe very slight or even no drop of the conductivity around the melting point. Especially for more viscous solutions corresponding to higher salt concentration (being of technological interest), the conductivity seems to follow the same VTF-like equation. That suggests that the polymer remains in its amorphous state thanks to the presence of the ceramic matrix. One of the most promising results is found with a concentrated salt solution in higher molecular weight polymer (PEODME1000 and PEO1e5). Ambient temperature conductivity is close to the technological limit (10^{-4} S·cm^{-1}) and is still subject to optimization.

For regular composite systems (ceramic-in-polymer), combined EIS and rheology studies showed that application of

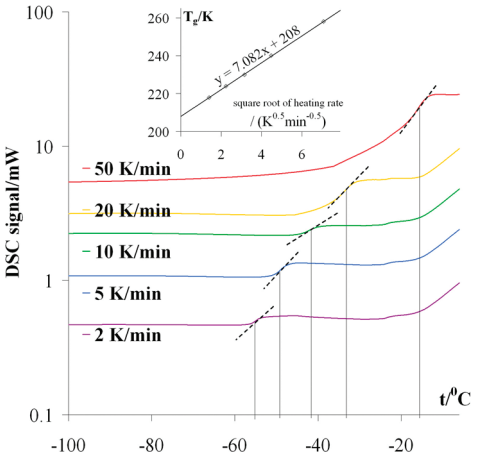

Figure 3. Thermograms showing the glass to elastomer transition for non composite electrolyte containing 1 mol·kg^{-1} of salt as observed at different heating rates. Inset shows linear extrapolation to zero heating rate. Dashed lines represent tangents at inflection points.

ceramic filler leads to an increase of viscosity but at the same time an enhancement of conductivity is observed as well as an increase of the cation transport number.[64] That suggests that when polymer and ceramic phase are in contact, the mechanism of conduction may be disturbed because of a different potential landscape near ceramic phase. Unlike powder-filled electrolytes, reversed-phase systems rheology cannot be studied; therefore, to address such alterations, Almond−West formalism was applied (description of the procedure can be found in refs 65−71; a detailed discussion will be published elsewhere). Calculations adapted to non-Arrhenius systems (according to the universal character of dielectric response[72]) showed that composites, as compared with noncomposite references, are characterized by lower pseudo-activation energy for conduction in the entire temperature range. Above the melting point the predominant factor is the decrease of the activation energy for charge carriers formation, below the melting point increase of charge carriers mobility seems to dominate. Fitting of the conductivity logarithm vs reciprocal temperature curves with VTF-like equation bore not only pseudo activation energies but also so-called thermodynamic glass transition temperatures (denoted T_0 as opposed to DSC-based values denoted T_g). They are provided as Supporting Information.

Differential Scanning Calorimetry. Poly(oxyethylene) exhibits two phase transitions: glass transition around 210 K (∼independent of the molecular weight) and melting, which appears around 280 K for 500 g·mol^{-1} olygomer and on increasing the molecular weight can reach 343 K for 5 × 10^6 g·mol^{-1} polymer. To satisfy recent recommendations in determining glass transition temperatures,[73] very consistent procedures were applied, namely, recording the thermograms at several heating rates and extrapolating the results to 0 K/min rate, taking care about the cooling rate in the preceding scan and using similar amounts of sample each time. Figure 3 presents a set of thermograms showing the glass to elastomer transition for a non-composite electrolyte containing 1 mol·kg^{-1} of salt as observed at different heating rates. Inset shows linear extrapolation to zero heating rate. Dashed lines represent tangents at inflection points. We observed that an increase of the heating rate causes an increase of the glass transition temperature as observed by DSC and moves it further and further away from the T_0 value extracted from VTF fitting of the conductivity data (as well as VTF

dx.doi.org/10.1021/cm103021r |Chem. Mater. 2011, 23, 1785–1797

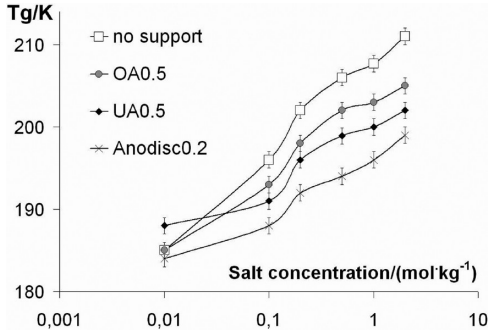

Figure 4. Plot of zero-heating rate glass transition temperatures as a function of salt concentration and type of sample (OA0.5, sample prepared with the help of pore-forming agent; UA0.5, ceramic pieces formed by uniaxial pressing, Anodisc0.2, the commercial alumina piece).

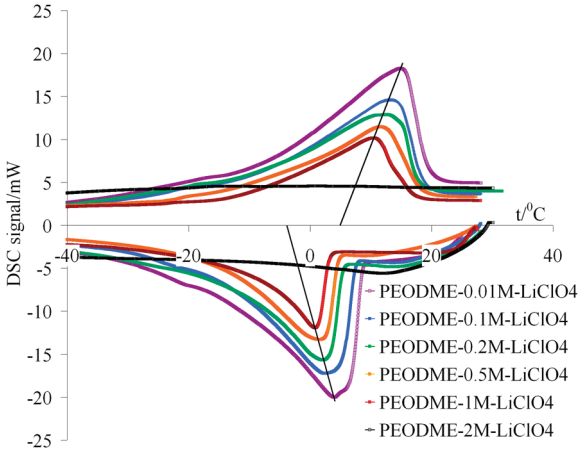

Figure 5. Melting peak for one of the systems under study as observed by DSC.

fitting of the viscosity data). At 50 K min^{-1}, it overlaps with the melting peak. At 2 K·min^{-1}, the signal becomes very weak, near the detection limit. To extract the zero heating rate value, we used a probability test to find system in which data follows a straight line and then used the intercept with ordinate axis.

Coming to the results themselves, we've observed that the glass transition temperature of the polyether depends on the salt concentration (Figure 4). This stays in good agreement with what can be found in the literature regarding the mechanism of conduction. Polymer contains electrodonor oxygen atoms in its structure, that are capable of coordinating species of Lewis acid character. When salt is dissolved into the polymer it dissociates partially, creating free ions, ion pairs, ionic triplets and higher aggregates. Lithium cations (Li^+) and positively charged triplets (e.g., $Li_2ClO_4^+$) can act as transient cross-links of the polymeric chains, thus restricting their movement. Numerous experiments showed, that in amorphous systems ionic conduction above the glass transition temperature is coupled with the segmental motion of polymeric chains. Since the increase of salt concentration restricts that movement more and more, in spite of increasing the salt concentration (and the dielectric constant sometimes), the conductivity increases only until certain point when it reaches its maximum (usually around 1 mol of salt per 1 kg of polymer) and then drops abruptly due to lowering of the polymeric matrix flexibility and aggregation of ions decreasing the effective charge carriers concentration.

When the polymer electrolyte is introduced into the ceramic, the glass transition temperature decreases in comparison with its bulk counterpart (Figure 4), suggesting that the amorphous phase is more flexible as suggested by de Gennes theory.[74−82] That would in turn imply, that its specific ionic conductivity could be enhanced. This agrees well with the results. For some composite samples conductivities measured at temperatures above the melting point were slightly higher than those of electrolyte solutions. Keeping in mind that an insulating alumina phase occupied a large fraction of samples these results are very interesting and prove that such materials are capable of providing exceptional functional properties when optimized. Interestingly, the T_0 values coming from VTF fitting show a little scatter around the value obtained for the noncomposite reference, and no clear trend is observed. This would in turn imply, that in some extent the conductivity is decoupled from the viscoelastic behavior of the polymer. Owing to the great surface area of the ceramic piece, such alteration of conducting mechanism is likely to occur.

Moving on to the other transition observed by DSC, that is, melting and crystallization, we have observed that the heat of melting and crystallization decreases as the concentration of salt increases (figure 5) and ultimately at 2 mol·kg^{-1} of salt, melting, and crystallization peaks disappear. Surprisingly, specific crystallization and melting heat is usually higher when polymer is supported by the ceramic piece, suggesting an increase in the crystallinity index. The latter was calculated with respect to the heat of melting of PEO reported in literature according to widely accepted procedure by dividing the recorded specific heat of melting by the heat of melting of highly crystalline reference. The effect is more pronounced as the pore size decreases as long as they are distributed randomly. In case of well-defined geometry the heat of melting and crystallization was lower, giving birth to lower crystallinity indexes. Detailed data is given in the Table S3 in Supporting Information. Because of the broad and complex character of the melting and crystallization peaks, temperatures corresponding to respective maxima/minima are reported, not the onsets. Nevertheless some lowering of the melting temperature with decreasing the pore size was observed as predicted by Hoffman's law[83] ($n^* = (2\sigma T_f^0)/(\Delta_m H^0(T_f^0 - T))$) ($n^*$ is the thickness of the crystal crystallized at temperature T, which is lower than the equilibrium melting point of infinitely large crystal (T_f^0), σ is the excess surface free energy associated with folded chains at the lateral surface of platelet crystals, $\Delta_m H^0$ is the heat of melting per one mer of polymer) emerges when looking at the thermograms of composites and references. It is difficult to judge however if there is any direct link between the pore size and melting temperature since for anodized alumina characterized by 20, 100, and 200 nm pore size, the differences in the melting peak shape and position are extremely little, nothing similar to results showed by Bishop et al.[47] was observed (Table S3, Supporting Information). In house prepared ceramics were characterized by very broad range of pore sizes thus concluding about any relationship between pore size and melting point might be difficult. Such observation may mean that the thickness of the crystals formed within the porous structure is smaller than the pore size; hence, there is no direct link between the two parameters. These results are different from classical composites, for which the changes of the glass transition temperature are similar (though less pronounced), however the heat of melting decreases upon addition of filler.[45,84,85]

dx.doi.org/10.1021/cm103021r |*Chem. Mater.* 2011, 23, 1785–1797

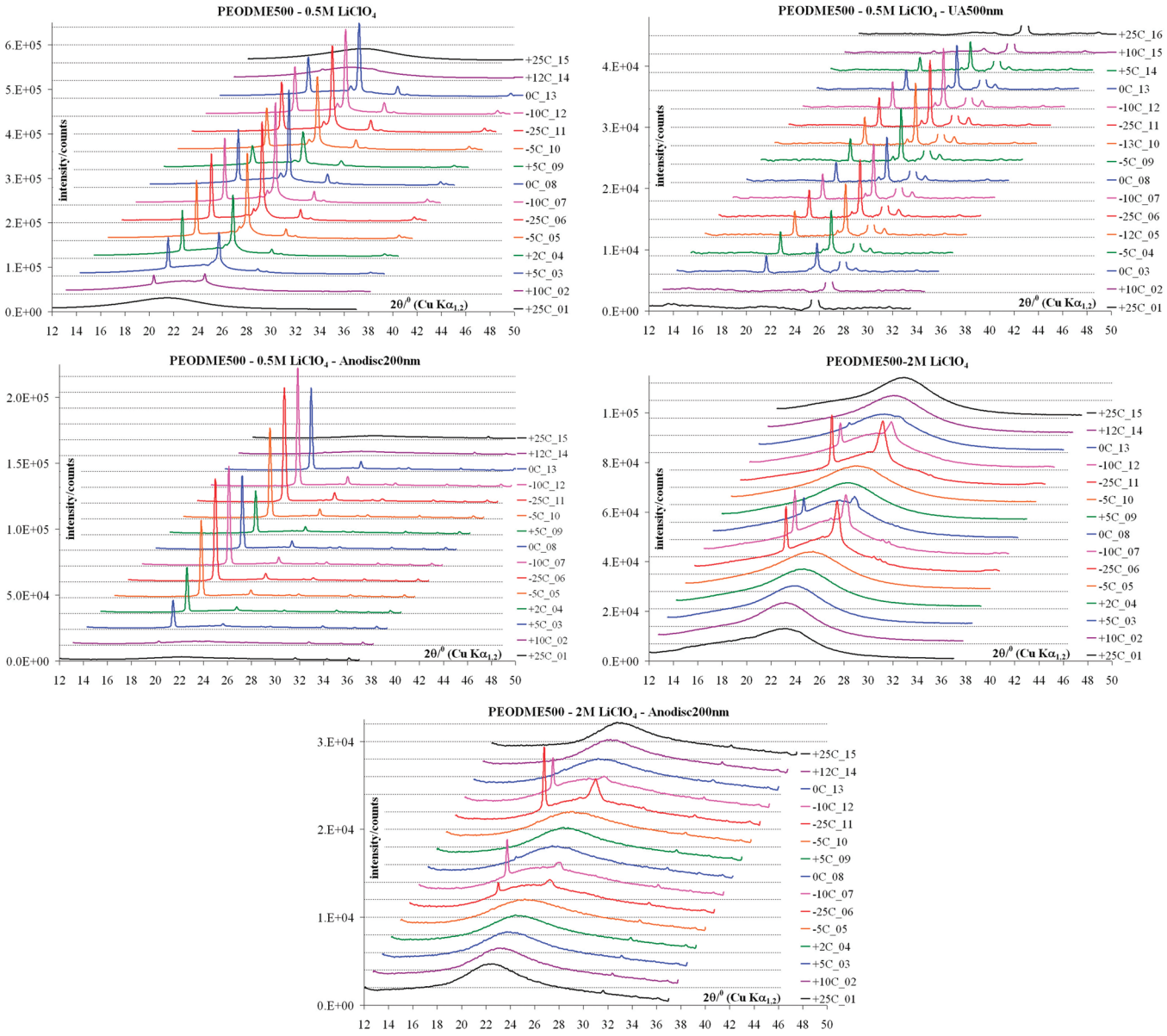

Figure 6. Environmental XRD studies of several samples. Legends on the right show the temperature at which specific diffractogram was recorded, the second number indicates the chronology: (a) noncomposite system, 0.5 M salt concentration; (b) composite based on UA0.5 ceramics (tiny, randomly oriented pores), 0.5 M salt concentration; (c) composite based on AN0.2 ceramics (200 nm pores, oriented perpendicularly to electrodes), 0.5 M salt concentration; (d) noncomposite system, 2 M salt concentration; (e) composite based on AN0.2 ceramics (200 nm pores, oriented perpendicularly to electrodes), 2 M salt concentration.

X-ray Diffraction. To study the phase transformations in further details, a more straightforward method was applied, namely, XRD experiments were performed for the polymer-in-ceramic and noncomposite systems. X-ray diffraction patterns were recorded as a function of temperature. Several cooling—heating cycles were performed to observe any irreversibilities. According to the DSC thermograms (Figure.5), several specific temperatures were selected for recording the patterns. It appeared that some reflections, especially in the low-angle zone, emerge from the amorphous halo at temperatures exceeding by a few K the point at which the crystallization peak begins in DSC. The same is valid for heating scans, that is, at temperatures exceeding the end of the melting peak, the low angle reflection is still visible, therefore claiming that it is just a kinetic effect is a vain. This would mean, that first steps of ordering of the polymer structure take place without detectable energetic effect.

Figure 6a—e presents results of environmental XRD studies of several samples. As can be seen, noncomposite sample and composite based on ceramic with randomly distributed pores are alike (for composite the Al_2O_3 reflection has been removed to clear up the picture (its intensity is about 60k counts) as a brief comparison with the previous figure shows there are no polymer reflections there). However for anodized alumina the behavior is different, that is, low angle reflection is much more intense at both salt concentrations. Furthermore it can be seen that XRD shows some crystallinity at 2 M salt concentration, whereas almost no clear melting/crystallization peaks were observed by DSC for same samples.

dx.doi.org/10.1021/cm103021r |*Chem. Mater.* 2011, 23, 1785–1797

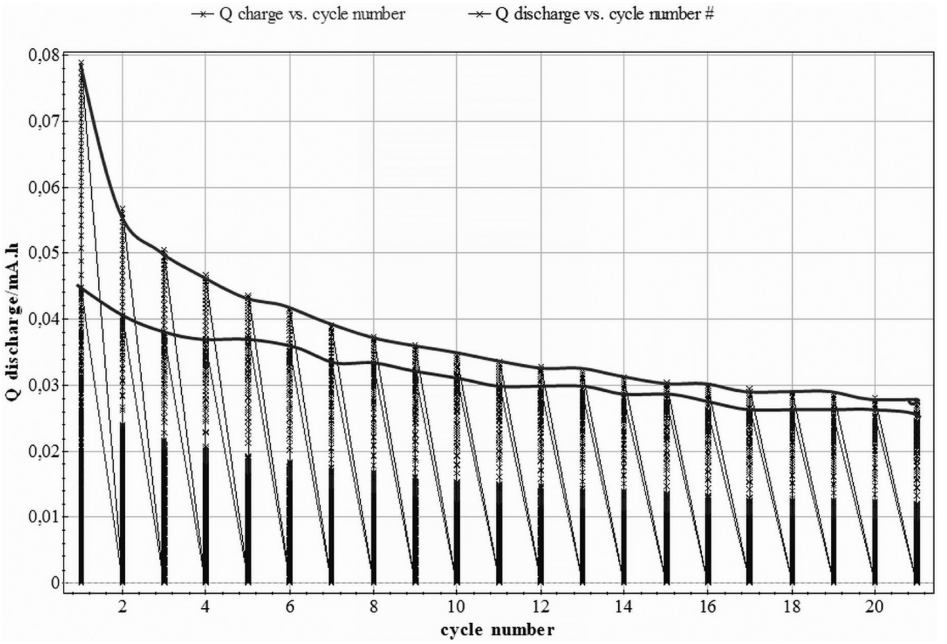

Figure 7. Galvanostatic cycling of ceramic piece based half cell. Electrodes: metallic Li (−), NiO−C composite (+) deposited on the electrolyte support Electrolyte: 1 M LiClO4/PEODME500 supported by anodized alumina membrane (200 nm pore size). Coin cell (CR2032) configuration.

At low salt concentration there are four reflections visible for all kind of samples (Figure 6a−c). They correspond to the *d*-spacings of 4.58, 3.78, 3.34, and 3.24 Å, respectively. Their positions remain almost unchanged upon temperature changes. When moving on to the relative intensities of these reflections it has to be pointed out, that usually the reflection at 3.78 Å is the most intense. The next one is that at 4.58 Å with relative intensity ranging from 40 to 70%. Those of 3.34 and 3.24 Å lie within 8−18% and 1 to 3%, respectively. However, in case of the commercial alumina sample, the preferred orientation caused by the parallel character of pores changed the intensities order into: 100%, 5−7%, 0.5−1%, 1.5−2.5% sequence respectively, as the *d*-spacings decrease. Furthermore the largest spacing was always larger by 1% than that observed for other composite samples, as well as the noncomposite system.

At high salt concentration the differences among the samples were more visible (figure 6 d, e). For all systems the intensities changed with the *d*-spacing in a similar manner as in case of anodized alumina-supported samples with low concentration electrolytes. The only difference was that the intensity of the 3.78 Å reflection was around 70%. For unfilled systems as well as those with no preferential orientation, the low angle reflection appeared at around 4.54 Å, and for the sample with vertical pores it was 4.63 Å, that is, it was larger by almost 2%. Furthermore in case of this sample, the 3.34 and 3.24 Å reflections were invisible, however a new one appeared at 2.83 Å, with relative intensity of 25−30%. Since exact determination of the space group and atomic positions within the cell for polymers is a challenge itself, this will be the subject of our future studies, however this simple phenomenological analysis shows clearly that supporting the polymer by porous ceramic makes it behave in a different manner. Furthermore variations of the morphology of the ceramic piece have direct implications on the polymer structure.

Apart from the changes of the structure of the crystalline phase also its amount was evaluated (Table S4 in Supporting Information). According to well-established procedures, relative crystallinity indexes were calculated as a ratio of the integrated intensity of crystalline phase reflections to the area of the amorphous background. Since this is a comparative study dealing with only one material (PEO) being the main component of all studied phases, we did not correct the results for angular dependence of absorption/beam profile, for the Lorentz polarization factor which is also angularly dependent or the multiplicity of planes in crystal. Separate tests showed that there is no interference of reflections originating from the alumina and from the electrolyte. For comparison of the crystallinity scans performed at −25 °C were used. This temperature is below all the crystallization peaks seen in DSC and the baseline is reached. Furthermore the XRD patterns for unfilled ceramic pieces were recorded at −25 °C for the sake of removing the background coming from the piece itself (hence alumina reflections and detector background were subtracted prior to calculations and were not included neither in the amorphous background nor in the crystalline peaks area). Using exactly the same temperature allows us to discriminate any thermal expansion corrections in the patterns. The relative crystallinity indexes calculated on the basis of XRD (Table S4) are different from that obtained by DSC (Table S3) but since both methods are based on different assumptions and material properties such differences are not strange and are widely described in textbooks. The more important than values are the trends that are very similar as observed by both, so much different methods. One can observe that at lower salt concentration the crystallinity of solidified electrolyte is higher when supported by the ceramic, on the other hand at higher salt concentration the reverse is true.

Another interesting fact is that crystallinity index, as we could actually expect looking at DSC curves, does not take its value just after passing the melting point and remain constant, but actually changes gradually. Figure S3 (a−d; Supporting Information) presents changes in the relative crystallinity index (as referred to the maximum reported for each sample) as a function of thermal history. For low viscosity system (0.5 M; a, b) the hysteresis loop

is much more narrow than for 2 M electrolytes (c, d). For composite system with high viscosity electrolyte (d), only second cooling leads to crystallinities similar to those of noncomposite counterparts. Even slow cooling did not allow the fresh sample to crystallize completely in this case. Increase of the crystallinity on first heating (from −25 °C to −10 °C) is a clear indication of this fact. Figure S4 (a, b; Supporting Information) presents the percentage of the maximum crystallinity calculated by DSC and XRD as a function of temperature for two systems under study. In general XRD bears much greater values and as can be seen, especially in the cooling scan XRD shows crystallization before any detectable thermal effect occurs (100% in panel a means 26% of crystallinity for DSC and 67% for XRD; data rescaled to 100% for more direct comparison). To recapitulate: structural changes depend strongly on the type of ceramic piece and on the salt concentration. The thermal history also matters as can be clearly seen.

Battery Cycling. Applicability of such composite electrolytes in an operational lithium cell was proven by testing NiO−C composite electrodes versus lithium metal (Figure 7). Potential window for cycling was determined by performing cycling voltammetry and was set to be 0.10−1.50 V. The current value was adjusted to get full material capacity in one hour. Prolonged cycling showed promising capacity retention, proving that the concept of ceramic-supported electrolyte (and in result whole battery) is feasible, as well as the new process for obtaining composite electrodes by application of microwave plasma to be capable of depositing electrodes on virtually any kind of substrate, regardless its morphology. Furthermore, no shortcuts were observed on the cycling the cells hence safety factor of such systems should be emphasized. Studies employing other active materials and reaction mechanisms are ongoing.

DISCUSSION

Combining the conductivity and structure information presented above a quite complex picture of these materials emerges. First of all the most astonishing result is the fact that the crystallinity of the polymer phase actually increases upon introduction into the ceramic support. Then, despite the increase of the crystallinity, below the melting point conductivities of composites are greater than those of noncomposite references. A brief look on the literature suggests that one possibility is the creation of some conductive crystalline phases as reported by Bruce et al.[86−88] That might be one explanation, however XRD results usually show the same set of reflections for both types of systems (with and without ceramic). That would mean that crystalline conductive phases either are present in both or neither of cases. Furthermore high ionic conductivities for crystalline phases were obtained after doping with other salts, inducing defects. Such doping was not applied in this work.

But then why the Arrhenius plots of conductivity are neither straight lines nor continuations of VTF-like curves from the high temperature zone? Assuming that there are two phases (crystalline and amorphous PEO-salt complex) contributing to the ionic transport apart from the pure crystalline PEO (which is present according to the phase diagram), the conductivity of the system depends not only on the conductivities of each phase but also on its volume fraction and topology. To illustrate this fact a simple diagram (Scheme 2) is provided. In situation A, the total conductivity is close to zero; in situation B, it is practically identical to the intrinsic conductivity of the conductive phase. In situation C, conductivity is of course lower than in case B, but it still is much greater than in the case A, although the content of the conductive phase is much lower. Hence the conclusion could be following. Noncomposite electrolytes can find the crystallization centers mainly on the surfaces, where they are in contact with solids (this might be a container, electrode, etc.). Therefore a lot of crystalline phase is created in the place of contact with current collectors. Assuming that these crystalline phases are poor conductors (what is usually the case, unless we carefully design the crystalline phase) it gives birth to high impedances. On the other hand, growing crystallites leave some amorphous phase in the center of the sample in the conductivity cell, or on its top when it is in the DSC crucible or on the cold stage of the X-ray diffractometer. That makes the measured crystallinity indexes low and system resembles situation A on the scheme. In composites the ceramic piece acts as a continuous center for crystallization, therefore ordering can take place simultaneously in the whole volume of the sample. This gives two results. First, a lot of grain boundaries are created that can conduct very well. Second, if we assume that the crystallization takes place from the walls of the pore toward its center, amorphous phase remaining in the centers of the pores, creates a network resembling the pore structure. Furthermore crystalline phase is characterized by greater density than the amorphous one hence polymer while crystallizing on the pore walls, leaves extra space for the remaining material. This creates mechanical forces acting toward expansion of the polymer. Results of these forces can be observed either by XRD that shows greater interplanar distances in the crystalline phases, or by mechanical properties. Such an in situ induced strain in the polymer results in further enhanced resistance against external force. Excellent mechanical strength of the composites seem to support our assumptions. Yet another observation is that the amorphous phase itself might be expanded by these forces. This means extra free volume which transforms into greater conductivity and lower glass transition temperature that was also observed experimentally. We suppose that extra forces might be also a reason for creation of new crystalline phase of more open structure that might contribute to the ionic transport (for one of the systems we observed a major change of large angle reflections).

Scheme 2. Possible Topologies of Samples

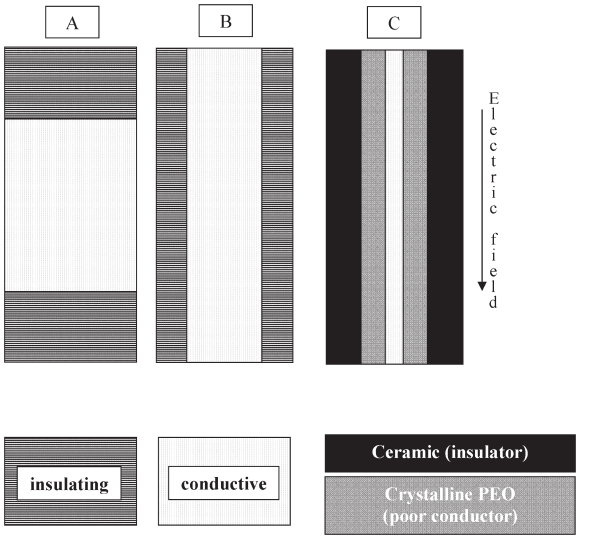

Nevertheless, since the pores are of open nature, such a network of amorphous phase, even if limited in volume, can percolate across the sample resulting in enhanced conductivity at sub ambient temperatures. Hence composite resembles something in between situation B and C on Scheme 2. Another proof can be the fact that as the viscosity of the electrolyte increases, increase in the pore size leads to better conductivities. Since crystallization of very viscous solutions takes time, provided that the pores are wide, a lot of amorphous phase can remain in the centers of the pores and create the percolating network easier.

Yet another proof that ceramic phase acts as a crystallization center and that the phase formed at the interface is a poor conductor may be found either in our previous works dealing with conductive particulate fillers (i.e., NASICON) where large interfacial resistance prohibited taking advantage of the conductivity of the filler itself,[19] as well as some molecular dynamics modeling works showing that the movement of lithium or polymer next to the ceramic is extremely limited as opposed to enhancement observed far away from the interface.[89,90]

The clear discrepancy of the melting temperature results between our and previously published results[47] may originate from several factors. These might be the little differences in the systems under study (pore sizes, type of salt) or in the preparation conditions. Taking into account our previous findings published recently,[91] it seems that having moisture in the system where as fragile polymer as PEO is in contact with ceramic surface that bears acidic sites of Lewis or Brønsted character, can lead to its degradation, which is more and more pronounced as the specific surface increases (decrease of the pore size). That could be sufficient to lead to the observed decrease of the melting point.

Results published previously show that in polymer systems (low dielectric constant) enhancement of interfacial stability vs low potential electrodes goes hand in hand with growth of the lithium transference number. This study shows the same trend. Since the salt decomposition is suspected to be the main event taking place at the interface, probably the salt−ceramic interactions are also pronounced. Spectroscopic investigations of ceramic-in-polymer analogues proved such interactions to be important.[92] Technical difficulties disabled us from conducting similar studies for reversed phase composites at this step.

CONCLUSIONS

A new class of materials has been presented, namely polymer-in-ceramic composite electrolytes. These reversed phase composites offer excellent and unusual mechanical properties: high rigidity combined with quasi-elasticity at high strains (insensitivity to brittle cracking). Thanks to the confinement of polymer in the pores (decrease of the glass transition temperature), conductivities above polymer melting point are very similar to those characteristic of noncomposite systems in spite of the fact, that electrolyte occupies only about 50% of the composite volume. Below the melting point, the disturbance of the crystallization process provoked by the ceramic phase leads to conductivity enhancement by up to 2 orders of magnitude. The mechanism of crystallization has yet to be fully understood, since results given by DSC, XRD, and conductivity measurements cannot be explained uniquely at this stage of the research project. As determined by appropriate calculations, it was found that activation energy of both charge carrier migration and creation is lowered by introduction of the ceramic phase, each factor playing a different role depending on the temperature range (below or above the melting point).

These systems offer good stability against lithium metal electrodes which is also important from the technological point of view. The safety issues that the lithium technology is facing seem to be possible to solve with the technology presented herein. Although enhancement of conductivity as well as increased stability against lithium metal can be obtained by addition of ceramic powders, the regular phase systems when capable of providing that high conductivity at ambient temperatures, lack mechanical stability. Furthermore, even if a thermal even occurs and the polymer phase disappears, there is still alumina separating the electrodes. In such a case electrodes will decompose separately and the damage to the user and environment will be surely less severe than with any present technology. One of the features making this technology feasible is the possibility of depositing the electrode material with plasma or high temperature processes directly on the electrolyte support, without any current collector that can be added afterward. Therefore the reversed phase systems are seen as a promising perspective for all-solid-state battery technology. Our findings on how to further enhance the performance of lithium metal electrodes based on particulate fillers might be easily applied in these reverse phase composites. Such works combined with exploration of all the prospects of this class of materials, as well as understanding the mechanisms involved are ongoing and are to be published in due time.

ASSOCIATED CONTENT

Supporting Information. Detailed description of some methods, procedures, and supplementary results. This material is available free of charge via the Internet at http://pubs.acs.org.

AUTHOR INFORMATION

Corresponding Author

*E-mail: jsyzdek@lbl.gov. Tel.: +1 510 486 4678. Fax: +1 510 486 7303.

ACKNOWLEDGMENT

This research project was realized within ALISTORE European Research Institute in collaboration with Special Ceramics Research Group from Warsaw University of Technology, Faculty of Chemistry. Staff from Laboratoire de Réactivité et de Chimie des Solides (Amiens), Special Ceramics Research Group and Polymer Ionics Research Group (Warsaw), is acknowledged for fruitful discussions and help with multiple experiments. J.S. thanks the European Union for its support in the framework of European Social Fund through the Warsaw University of Technology Development Program.

REFERENCES

(1) Fenton, D. E.; Parker, J. M.; Wright, P. V. *Polymer* **1973**, *14*, 589.
(2) Wright, P. V. *Br. Polym. J.* **1975**, *7*, 319–327.
(3) Wright, P. V. *Electrochim. Acta* **1998**, *43*, 1137–1143.
(4) Armand, M. B., Ed.; In *Solid Electrolytes: General Principles, Characterization, Materials, Applications*; Academic Press: New York, 1978; Vol. 4, pp 251−252.
(5) Armand, M. B.; Chabagno, J. M.; Duclot, M. J. *Fast Ion Transp. Solids: Electrodes Electrolytes, Proc. Int. Conf.* **1979**, 131–136.
(6) Fenton, D. E.; Parker, J. M.; Wright, P. V. *Polymer* **1973**, *14*, 589.
(7) Wright, P. V. *Br. Polym. J.* **1975**, *7*, 319–327.

(8) Armand, M. B. New Electrode Material. *Fast Ion Transport in Solids, Solid State Batteries and Devices*, Proceedings of the NATO Sponsored Advanced Study Institute on Fast Ion Transport in Solids, Solid State Batteries and Devices, Belgirate, Italy, 5−15 September 1972; van Gool, W., Ed.; North Holland Publishing Company: Amsterdam, 1973.
(9) Fenton, D. E.; Parker, J. M.; Wright, P. V. *Polymer* **1973**, *14*, 589–589.
(10) Marcinek, M.; Zalewska, A.; Zukowska, G.; Wieczorek, W. *Solid State Ionics* **2000**, *136−137*, 1175–1179.
(11) Tarascon, J. M.; Armand, M. *Nature* **2001**, *414*, 359–367.
(12) Croce, F.; Sacchetti, S.; Scrosati, B. *J. Power Sources* **2006**, *162*, 685–689.
(13) Florjanczyk, Z.; Marcinek, M.; Wieczorek, W.; Langwald, N. *Pol. J. Chem.* **2004**, *78*, 1279–1304.
(14) Goodenough, J. B.; Hong, H. Y.; Kafalas, J. A. *Mater. Res. Bull.* **1976**, *11*, 203–220.
(15) Gray, F.; Armand, M. *Handb. Battery Mater.* **1999**, 499–523.
(16) Sebastian, L.; Gopalakrishnan, J. *J. Mater. Chem.* **2003**, *13*, 433–441.
(17) Kafalas, J. A.; Hong, H. Y. P. *Proc. Power Sources Symp, 28th*, 1978, 1−2.
(18) Hooper, A. *J. Phys. D: Appl. Phys.* **1977**, *10*, 1487–1496.
(19) Plocharski, J.; Wieczorek, W. *Solid State Ionics* **1988**, *28−30*, 979–982.
(20) Wieczorek, W.; Such, K.; Wycislik, H.; Plocharski, J. *Solid State Ionics* **1989**, *36*, 255–257.
(21) Villarreal, I.; Morales, E.; Acosta, J. L. *Angew. Makromol. Chem.* **1999**, *266*, 24–29.
(22) Sun, H. Y.; Takeda, Y.; Imanishi, N.; Yamamoto, O.; Sohn, H. *J. Electrochem. Soc.* **2000**, *147*, 2462–2467.
(23) Capiglia, C.; Yang, J.; Imanishi, N.; Hirano, A.; Takeda, Y.; Yamamoto, O. *Solid State Ionics* **2002**, *154−155*, 7–14.
(24) Przyluski, J.; Wieczorek, W. *Solid State Ionics* **1989**, *36*, 165–169.
(25) Wieczorek, W.; Such, K.; Chung, S. H.; Stevens, J. R. *J. Phys. Chem.* **1994**, *98*, 9047–9055.
(26) Kumar, B.; Scanlon, L. G. *J. Electroceram.* **2000**, *5*, 127–139.
(27) Johansson, P.; Ratner, M. A.; Shriver, D. F. *J. Phys. Chem. B* **2001**, *105*, 9016–9021.
(28) Syzdek, J.; Armand, M. B.; Marcinek, M.; Zalewska, A.; Żukowska, G. Z.; Wieczorek, W. *Electrochim. Acta* **2010**, *55*, 1314–1322.
(29) Vaia, R. A.; Ishii, H.; Giannelis, E. P. *Chem. Mater.* **1993**, *5*, 1694–1696.
(30) Aranda, P.; Ruiz-Hitzky, E. *Chem. Mater.* **1992**, *4*, 1395–1403.
(31) Vaia, R. A.; Jandt, K. D.; Kramer, E. J.; Giannelis, E. P. *Macromolecules* **1995**, *28*, 8080–8085.
(32) Riley, M.; Fedkiw, P. S.; Khan, S. A. *J. Electrochem. Soc.* **2002**, *149*, A667–A674.
(33) Vorrey, S.; Teeters, D. *Electrochim. Acta* **2003**, *48*, 2137–2141.
(34) Riley, M. W.; Fedkiw, P. S.; Khan, S. A. *J. Electrochem. Soc.* **2003**, *150*, A933–A941.
(35) Vorrey, S.; Teeters, D. In *Enhanced ionic conduction in polymer electrolytes by confinement in nanoscale pores*; Meeting Abstracts: 205th Meeting of The Electrochemical Society, MA 2004 01; Electrochemical Society: Pennington, NJ, 2004; pp 359.
(36) Layson, A. R.; Teeters, D. *Solid State Ionics* **2004**, *175*, 773–780.
(37) Volel, M.; Armand, M.; Gorecki, W.; Saboungi, M. *Chem. Mater.* **2005**, *17*, 2028–2033.
(38) Sandí, G.; Kizilel, R.; Carrado, K. A.; Fernández-Saavedra, R.; Castagnola, N. *Electrochim. Acta* **2005**, *50*, 3891–3896.
(39) Lee, L. J.; Zeng, C.; Cao, X.; Han, X.; Shen, J.; Xu, G. *Compos. Sci. Technol.* **2005**, *65*, 2344–2363.
(40) Castriota, M.; Teeters, D. *Ionics* **2005**, *11*, 220–225.
(41) Hoa, M. L. K.; Lu, M.; Zhang, Y. *Adv. Colloid Interface Sci.* **2006**, *121*, 9–23.
(42) Chen, H.; Palmese, G. R.; Elabd, Y. A. *Chem. Mater.* **2006**, *18*, 4875–4881.
(43) Kalyana Sundaram, N. T.; Vasudevan, T.; Subramania, A. *J. Phys. Chem. Solids* **2007**, *68*, 264–271.
(44) Zhou, J.; Fedkiw, P. S. *Solid State Ionics* **2004**, *166*, 275–293.
(45) Swierczynski, D.; Zalewska, A.; Wieczorek, W. *Chem. Mater.* **2001**, *13*, 1560–1564.
(46) Munch, E.; Launey, M. E.; Alsem, D. H.; Saiz, E.; Tomsia, A. P.; Ritchie, R. O. *Science* **2008**, *322*, 1516–1520.
(47) Bishop, C.; Teeters, D. *Electrochim. Acta* **2009**, *54*, 4084–4088.
(48) Syzdek, J.; Armand, M.; Gizowska, M.; Marcinek, M.; Sasim, E.; Szafran, M.; Wieczorek, W. *J. Power Sources* **2009**, *194*, 66–72.
(49) Kostecki, R.; Marcinek, M. Patent 2010005541, 2010.
(50) Marcinek, M.; Hardwick, L. J.; Richardson, T. J.; Song, X.; Kostecki, R. *J. Power Sources* **2007**, *173*, 965–971.
(51) Marcinek, M.; Song, X.; Kostecki, R. *Electrochem. Commun.* **2007**, *9*, 1739–1743.
(52) Kostecki, R.; Marcinek, M., Int. Patent WO/2006/130739, 2006.
(53) Agarwal, P.; Crisalle, O. D.; Orazem, M. E.; Garcia-Rubio, L. *J. Electrochem. Soc.* **1995**, *142*, 4149–4158.
(54) Agarwal, P.; Orazem, M. E.; Garcia-Rubio, L. *J. Electrochem. Soc.* **1992**, *139*, 1917–1927.
(55) Boukamp, B. A. *J. Electrochem. Soc.* **1995**, *142*, 1885–1894.
(56) Macdonald, D. D.; Urquidi-Macdonald, M. *J. Electrochem. Soc.* **1985**, *132*, 2316–2319.
(57) Vogel, H. *Phys. Z.* **1921**, *22*, 645–646.
(58) Tammann, G.; Hesse, W. *Z. Anorg. Allg. Chem.* **1926**, *156*, 245–257.
(59) Fulcher, G. S. *J. Am. Ceram. Soc.* **1925**, *8*, 339–355.
(60) Williams, M. L.; Landel, R. F.; Ferry, J. D. *J. Am. Chem. Soc.* **1955**, *77*, 3701–3707.
(61) Xu, P.; Mark, J. In *Filler-Polymer Bonding and Its Role in Elastomer Reinforcement*, Proceedings of the ACS Division of Polymeric Materials Science and Engineering; American Chemical Society: Washington, DC, 1993; Vol. 68, pp 285−286.
(62) Marcinek, M.; Ciosek, M.; Zukowska, G.; Wieczorek, W.; Jeffrey, K. R.; Stevens, J. R. *Solid State Ionics* **2005**, *176*, 367–376.
(63) Marcinek, M.; Ciosek, M.; Zukowska, G.; Wieczorek, W.; Jeffrey, K. R.; Stevens, J. R. *Solid State Ionics* **2004**, *171*, 69–80.
(64) Syzdek, J. S. *Application of Modified Ceramic Powders As Fillers for Composite Polymeric Electrolytes Based on Poly(oxyethylene)*; Oficyna Wydawnicza Politechniki Warszawskiej: Warszawa, Poland, 2009.
(65) Siekierski, M.; Wieczorek, W. *Solid State Ionics* **1993**, *60*, 67–71.
(66) Siekierski, M.; Wieczorek, W.; Przyluski, J. *Electrochim. Acta* **1998**, *43*, 1339–1342.
(67) Almond, D. P.; West, A. R. *Solid State Ionics* **1987**, *23*, 27–35.
(68) Almond, D. P.; West, A. R. *Solid State Ionics* **1986**, *18−19*, 1105–1109.
(69) Almond, D. P.; Duncan, G. K.; West, A. R. *Solid State Ionics* **1983**, *8*, 159–164.
(70) Almond, D. P.; West, A. R. *Solid State Ionics* **1983**, *9−10*, 277–282.
(71) Almond, D. P.; West, A. R.; Grant, R. J. *Solid State Commun.* **1982**, *44*, 1277–1280.
(72) Jonscher, A. K. *Nature* **1977**, *267*, 673–679.
(73) Mazurin, O. *Glass Phys. Chem.* **2007**, *33*, 22–36.
(74) de Gennes, P. G. *Phys. A Stat. Theor. Phys.* **1998**, *261*, 267–293.
(75) Adjari, A.; Brochard-Wyart, F.; de Gennes, P.; Leibler, L.; Viovy, J.; Rubinstein, M. *Phys. A (Amsterdam, Neth.)* **1994**, *204*, 17–39.
(76) Brochard-Wyart, F.; de Gennes, P. G. *Adv. Colloid Interface Sci.* **1992**, *39*, 1–11.
(77) de Gennes, P. G. *Adv. Colloid Interface Sci.* **1987**, *27*, 189–209.
(78) Joanny, J. F.; De Gennes, P. G. *J. Colloid Interface Sci.* **1986**, *111*, 94–101.
(79) Gennes, P. G. d. *Radiat. Phys. Chem.* **1983**, *22*, 193–196.
(80) De Gennes, P. G. The Formation of Polymer/Polymer Junctions. In *Tribology*; Microscopic Aspects of Adhesion and Lubrication, Proceedings of the 34th International Meeting of the Société de Chimie

Physique; Georges, J. M., Ed.; Elsevier: Amsterdam, 1981; Vol. 7, pp 355−367.
(81) Dubois-Violette, E.; De Gennes, P. G. *J. Colloid Interface Sci.* **1976**, *57*, 403–410.
(82) De Gennes, P. G. *Phys. Lett. A* **1969**, *30*, 454–455.
(83) Andrews, R. J.; Grulke, E. A. *Polym. Handb.* **1999**, 231.
(84) Sannier, L.; Zalewska, A.; Wieczorek, W.; Marczewski, M.; Marczewska, H. *Electrochim. Acta* **2007**, *52*, 5685–5689.
(85) Moskwiak, M.; Giska, I.; Borkowska, R.; Zalewska, A.; Marczewski, M.; Marczewska, H.; Wieczorek, W. *J. Power Sources* **2006**, *159*, 443–448.
(86) MacGlashan, G. S.; Andreev, Y. G.; Bruce, P. *Nature* **1999**, *398*, 792–793.
(87) Gadjourova, Z.; Andreev, Y. G.; Tunstall, D. P.; Bruce, P. G. *Nature* **2001**, *412*, 520–523.
(88) Zhang, C.; Gamble, S.; Ainsworth, D.; Slawin, A. M. Z.; Andreev, Y. G.; Bruce, P. G. *Nat. Mater.* **2009**, *8*, 580.
(89) Van Eijck, L.; Best, A. S.; Stride, J.; Kearley, G. J. *Chem. Phys.* **2005**, *317*, 282–288.
(90) Kasemägi, H.; Aabloo, A.; Klintenberg, M. K.; Thomas, J. O. *Solid State Ionics* **2004**, *168*, 249–254.
(91) Syzdek, J.; Armand, M.; Marcinek, M.; Zalewska, A.; Żukowska, G.; Wieczorek, W. *Electrochim. Acta* **2010**, *55*, 1314–1322.
(92) Marcinek, M.; Bac, A.; Lipka, P.; Zalewska, A.; Zukowska, G.; Borkowska, R.; Wieczorek, W. *J. Phys. Chem. B* **2000**, *104*, 11088–11093.